

# Silicon-Graphene Hybrid Slot Waveguide with Enhanced Four-Wave Mixing Efficiency

Yuxing Yang, Xinhong Jiang, Zhenzhen Xu, Yong Zhang,  
Ciyuan Qiu, Xuhan Guo, and Yikai Su

State Key Lab of Advanced Optical Communication Systems and Networks, Department of Electronic Engineering  
Shanghai Jiao Tong University, Shanghai 200240, China  
[yikaisu@sjtu.edu.cn](mailto:yikaisu@sjtu.edu.cn)

**Abstract:** An enhanced four-wave mixing in a silicon-graphene hybrid slot waveguide is proposed and experimentally demonstrated. The conversion efficiency is  $-48.8$  dB, showing 3.2-dB and 0.5-dB improvements relative to silicon slot waveguide and strip waveguide, respectively.

**OCIS codes:** (130.3120) Integrated optics devices; (190.4380) Nonlinear optics, four-wave mixing

## 1. Introduction

Four-wave mixing (FWM) has been widely investigated to implement all-optical signal processing functions such as signal amplification, wavelength conversion, optical logic gate, and optical sampling [1–4]. To achieve high-efficiency FWM, silicon photonic devices with high nonlinear parameters have been studied due to their compact footprints and compatibility with the complementary metal-oxide-semiconductor (CMOS) process. However, the two-photon absorption (TPA) and TPA-induced free-carrier absorption (FCA) in the silicon limit the efficiency and the speed of the FWM. A silicon-organic hybrid waveguide, which consisted of a silicon slot waveguide filled and surrounded by a nonlinear organic cladding, was demonstrated with a high nonlinearity and also avoided the speed limitation of FCA [5]. Thus, combining the silicon slot waveguide with a high nonlinear material may become a promising way to implement high-speed and high-efficiency FWM.

Graphene, a single sheet of carbon atom in a hexagonal lattice, has generated tremendous interests in optoelectronics and photonics due to its gapless bandgap structure. Recently, Z-scan method was used to measure the high nonlinear Kerr coefficient of graphene [6]. Many studies have been carried out to integrate the graphene sheets with the nonlinear devices, such as nonlinear fibers and silicon photonic devices [7, 8]. However, in the case of a silicon slot waveguide with a narrow slot width, the graphene was difficult to fill into the slot by traditional poly (methyl methacrylate) (PMMA)-assisted wet-transfer method [9]. In our previous study [10], we have reported a bottom-up approach to grow the graphene directly on silicon/silica substrate, and demonstrated that the Kerr coefficient of the prepared graphene is  $10^{-12} \text{ m}^2 \text{ W}^{-1}$ .

In this paper, we propose and demonstrate a silicon-graphene hybrid (SGH) slot waveguide based on the bottom-up fabrication approach so that the graphene can be easily grown in the silicon slot waveguide. Benefitting from strong light-material interaction in the highly confined slot region filled with the graphene, an enhanced FWM using the proposed SGH slot waveguide is experimentally demonstrated. The conversion efficiency of the proposed SGH slot waveguide is  $-48.8$  dB, which is increased by 3.2 dB compared with the silicon slot waveguide, and 0.5 dB relative to the silicon strip waveguide.

## 2. Device design and fabrication

The proposed SGH slot waveguide is schematically illustrated in Figs. 1(a) and 1(b), which consists of two closely spaced silicon waveguides separated by a narrow slot. At the two ends of the slot waveguide, the widths of the slot have been tapered over a  $6\text{-}\mu\text{m}$  lengths to form strip waveguides, which are connected to TE-polarization grating couplers for coupling the light in and out of the chip. The silicon slot waveguide is filled and surrounded by a graphene-silica nanomaterial grown by our previously reported method [10]. The simulated electric field distribution of the quasi-TE mode of the SGH slot waveguide is shown in Fig. 1(c). The simulation is performed by using a commercial mode solver (COMSOL Multiphysics 4.3a) based on finite element method (FEM). In the simulation, the cross-section of the silicon core is  $220 \times 220 \text{ nm}^2$ , the width of the slot is  $150 \text{ nm}$ , and the thickness of the graphene-silica nanomaterial is  $360 \text{ nm}$ . The wavelength is set at  $\lambda = 1550 \text{ nm}$ . The refractive indices for the silicon and the silica are assumed to be  $n_{\text{Si}} = 3.455$ , and  $n_{\text{Silica}} = 1.445$ , respectively. The refractive index of the graphene-silica nanomaterial is assumed to be  $n_{\text{graphene-silica}} = 1.445$ , as the mass percentage of the graphene is lower than 1% [10].

From Fig. 1(c), it is clear to find that the electric field is strongly confined in the slot region filled and surrounded by the graphene-silica nanomaterial. The nonlinear parameter  $\gamma$  of the SGH slot waveguide is given by the following equation [11]:

$$\gamma = \frac{2\pi \iint S_z^2 n_2(x,y) dx dy}{\lambda (\iint S_z dx dy)^2}, \quad (1)$$

where  $S_z$  is the time-averaged Poynting vector and  $n_2$  is the nonlinear Kerr coefficient. The integrals are performed in the core and cladding materials with either the propagating or the evanescent electric field. According to Refs. [5] and [12], the nonlinear Kerr coefficients of the silicon, the silica, and the graphene-silica nanomaterial are assumed to be  $4.5 \times 10^{-18} \text{ m}^2 \text{ W}^{-1}$ ,  $3 \times 10^{-20} \text{ m}^2 \text{ W}^{-1}$ , and  $1 \times 10^{-12} \text{ m}^2 \text{ W}^{-1}$ , respectively. For the SGH slot waveguide, the value of  $\gamma$  is as high as  $1.5 \times 10^5 \text{ W}^{-1} \text{ km}^{-1}$ , which is higher than that of the silicon-polymer slot waveguide [5].

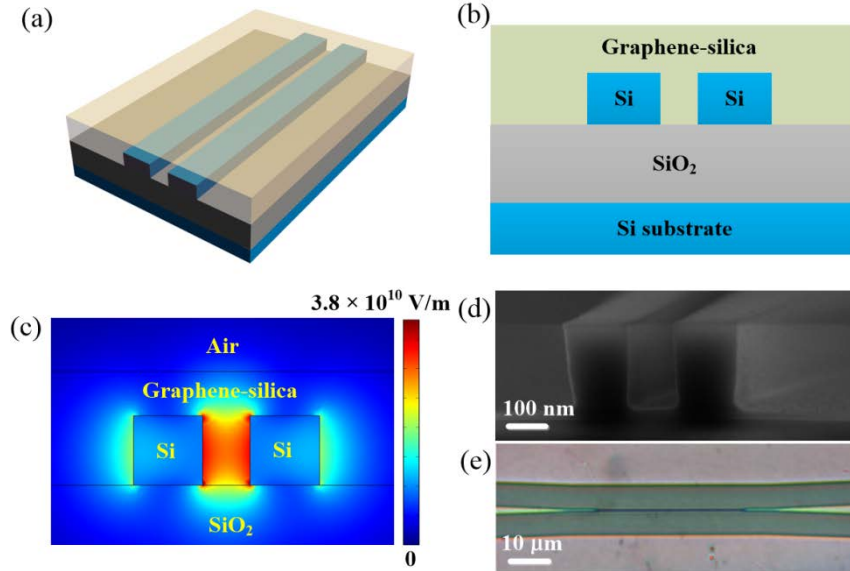


Fig. 1. Illustration of the proposed SGH slot waveguide. (a) 3D view. (b) Cross-section view. (c) Fundamental quasi-TE mode electric field distribution of the SGH slot waveguide. (d) SEM image of the silicon slot waveguide. (e) Optical micrograph of the SGH slot waveguide.

The proposed SGH slot waveguide was fabricated on a silicon-on-insulator (SOI) wafer with a 220-nm-thick top silicon layer. The silicon slot waveguide was defined by the processes of electron beam lithography (EBL) and inductive coupling plasma (ICP) etching. The cross-section of the slot region can be seen by the scanning electron micrograph (SEM) image in Fig. 1(d). After that, a solution, prepared by the bottom-up approach that consists of the silica and the pre-graphene, was spin coated on the silicon slot waveguide. Then, thermal treatment was carried out at 900 °C for 2 hours in a nitrogen flow to make the silicon slot waveguide filled and surrounded by the graphene-silica nanomaterial. The top view of the SGS device with the 40- $\mu\text{m}$ -length slot is shown in Fig. 1(e) under the optical microscope.

### 3. Experimental setup and results

Figure 2(a) illustrates the experimental setup for testing the degenerate FWM process with the SGH slot waveguide. For comparison purpose, a silicon slot waveguide device with the same parameters but without the graphene was also prepared and measured. Two tunable continuous-wave (CW) lasers are separately amplified by two erbium-doped fiber amplifiers (EDFAs; KEOPSYS CEFA-C-PB-HP and PriTel), and serve as the pump and signal sources, respectively. In each optical path, a tunable band pass filter (BPF) and a polarization controller (PC) are employed to suppress the sideband noise of the EDFA and to ensure the input light with TE-polarization. A 50:50 coupler is used to combine the pump and the signal lights, and then coupled to the device under test (DUT) through the TE polarization grating coupler. The output light is collected and measured by the optical spectrum analyzer (OSA; Yokogawa, AQ6370).

Here, the conversion efficiency of the FWM is defined as the ratio of the output idler power to that of the input signal [13]. The input power into the waveguide can be calculated by taking out the coupling loss from that of the input fiber. In our experiment, the length of the slot is 40  $\mu\text{m}$ . The coupling loss of a grating coupling system is 13 dB including two ends. Before coupled into the device, the pump power is set to 23 dBm at 1550 nm, and the signal

power is 15 dBm at 1549 nm. Thus the pump power at the waveguide input is estimated to be 16.5 dBm. The measured FWM transmission spectra for the silicon slot waveguide and the SGH slot waveguide are shown in Fig. 2(b), and a maximum conversion efficiency of  $-48.8$  dB is obtained with the SGH slot waveguide. From the zoom-in image in Fig. 2(c), the enhancement of conversion efficiency can be clearly observed. Compared with the silicon slot waveguide, the maximum conversion efficiency is increased by 3.2 dB with the 40- $\mu\text{m}$ -length slot. Furthermore, to compare with the standard silicon strip waveguide, we prepared such a device with the same waveguide height and 480-nm width without the slot, and the conversion efficiency of the silicon strip waveguide is  $-49.3$  dB. The SGH waveguide therefore shows higher nonlinearity with intrinsically fs-scale speed through the Kerr response.

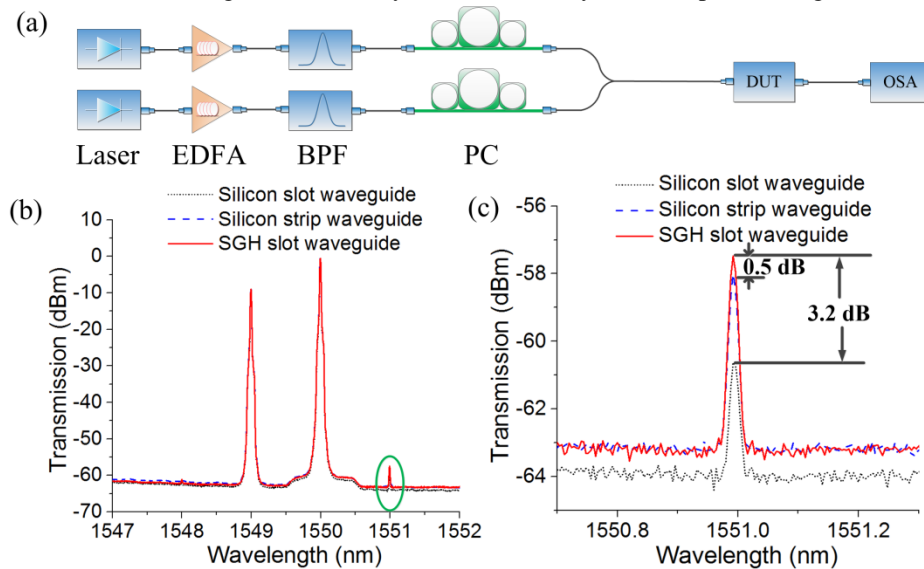


Fig. 2. (a) Experimental setup for testing degenerate FWM of the fabricated devices. (b) FWM spectra of the silicon slot waveguide (black dotted), the silicon strip waveguide (blue dashed), and the SGH slot waveguide (red solid). (c) zoom-in image of the idlers plotted using the green ellipse in (b).

#### 4. Conclusion

In summary, we have proposed and demonstrated a SGH slot waveguide based on the bottom-up fabrication process, which provides a new method to integrate the graphene to the silicon photonic devices on a large scale. At a pump power of 16.5 dBm into the waveguide, the FWM conversion efficiency of the SGH slot waveguide is  $-48.8$  dB, showing an improvement of 3.2 dB relative to the silicon slot waveguide, and 0.5-dB enhancement compared with the silicon strip waveguide. Such a silicon-graphene slot waveguide device may become a promising scheme to implement high-speed and high-efficiency FWM with mitigated TPA/FCA effects.

#### References

- [1] Stylianos Sygletos et al., "A novel method of pump and idler signal generation for non-degenerate FWM based phase sensitive amplification," *Lasers and Electro-Optic* **74**, 1-2 (2010).
- [2] Xiao Hu et al., "Graphene-silicon microring resonator enhanced all-optical up and down wavelength conversion of QPSK signal," *Opt. Express* **24**, 7168-7177 (2016).
- [3] Z. H. Li et al., "Ultra-high-speed reconfigurable logic gates based on four-wave mixing in a semiconductor optical amplifier," *IEEE Photon. Technol. Lett.* **18**, 1341-1343 (2006).
- [4] J. Li et al., "300-Gb/s eye-diagram measurement by optical sampling using fiber-based parametric amplification," *IEEE Photon. Technol. Lett.* **13**, 987-989 (2001).
- [5] C. Koos et al., "All-optical high-speed signal processing with silicon-organic hybrid slot waveguides," *Nature Photon.* **3**, 216-219 (2009).
- [6] Han Zhang et al., "Z-scan measurement of the nonlinear refractive index of graphene," *Opt. Lett.* **37**, 1856-1858 (2012).
- [7] K. K. Chow et al., "Four-wave-mixing-based wavelength conversion using a single-walled carbon-nanotube-deposited planar lightwave circuit waveguide," *Opt. Lett.* **35**, 2070-2072 (2010).
- [8] T. Gu et al., "Regenerative oscillation and four-wave mixing in graphene optoelectronics," *Nature Photon.* **6**, 554-559 (2012).
- [9] Xuelei Liang et al., "Toward clean and crackless transfer of graphene," *ACS Nano* **5**, 9144-9153 (2011).
- [10] Yuxing Yang et al., "Bottom-up fabrication of graphene on silicon/silica substrate via a facile soft-hard template approach," *Sci. Rep.* **5**, 13480 (2015).
- [11] Mengxi Ji et al., "Enhanced parametric frequency conversion in a compact silicon-graphene microring resonator," *Opt. Express* **23**, 18679-18685 (2015).
- [12] J. Leuthold et al., "Nonlinear silicon photonics," *Nature Photon.* **4**, 535-544 (2010).
- [13] M. A. Foster et al., "Broad-band optical parametric gain on a silicon photonic chip," *Nature* **441**, 960-963 (2006).